RESILIENT INFRASTRUCTURE
June 1–4, 2016
RESILIENT INFRASTRUCTURE LONDON 2016

FLEXURAL TESTS OF CONTINUOUS CONCRETE SLABS REINFORCED WITH BASALT FIBER-REINFORCED POLYMER BARS

Akiel, Mohammad
M.Sc. Candidate, United Arab Emirates University, UAE

El-Maaddawy, Tamer
Associate Professor, United Arab Emirates University, UAE

El Refai, Ahmed
Associate Professor, Laval University, Canada

ABSTRACT

Continuous steel-reinforced concrete slabs are vulnerable to corrosion damage and cracking. Non-metallic basalt fiber-reinforced polymer (BFRP) bars have a great potential to overcome corrosion problems. In this paper, test results of six continuous concrete slabs internally-reinforced with BFRP bars are reported. The specimens were divided into two groups based on the BFRP reinforcement ratio in the sagging regions ($2.5\rho_{fb}$ and $0.8\rho_{fb}$), where ρ_{fb} is the balanced reinforcement ratio of BFRP reinforcement. In each group, the hogging-to-sagging BFRP reinforcement ratio was 0.5, 0.72, or 1. Increasing the hogging-to-sagging BFRP reinforcement ratio increased the ultimate load but had almost no effect on the cracking load. The flexural response of continuous slabs that failed by rupture of BFRP bars was more sensitive to the hogging-to-sagging BFRP reinforcement ratio than that of the slabs that failed by concrete crushing. The moment redistribution ratio in the sagging region at failure of the later specimens was in the range of +40% to +48% compared to +10% to +26% for the former specimens.

Keywords: concrete, continuous, BFRP, flexure, redistribution, slabs

1. INTRODUCTION

The most dominant form of deterioration of steel-reinforced concrete structures is corrosion of steel reinforcement (El Maaddawy et al. 2005a, b). Non-corrosive fiber-reinforced polymer (FRP) bars have emerged as a result of the new technology in materials manufacturing. Because of their high strength-to-weight ratio, light weight, and high corrosion resistance, the use of FRP bars as replacement of traditional steel reinforcing bars is considered an ideal solution to eliminate corrosion problems in reinforced concrete structures (Bakis et al. 2002; Bank 2006). However, the ductility and deformability of FRP-reinforced concrete elements are questionable because of the linear-elastic response of FRP. Several studies were conducted to examine the flexural response of simply supported concrete elements internally reinforced with FRP bars (Kassem et al. 2011; Ovitigala and Issa 2013). Specimens reinforced with FRP bars exhibited greater deflections than those of their counterparts reinforced with steel bars. This was attributed to the reduced modulus of elasticity of FRP bars compared to that of steel, which resulted in larger cracks, reduced effective moment of inertia, and hence greater deflections. In evaluating the flexural capacity of FRP-reinforced concrete structures, concrete crushing at ultimate is generally preferable to the FRP rupture in order to prevent catastrophic failures and to ensure high degrees of deformability. Very little information is available in the literature on the performance of continuous concrete structures internally reinforced with FRP bars (El-Mogy et al. 2010; Habeeb and Ashour 2008). Moreover, the ACI 440.1R-06 (2006) does not allow moment redistribution in statically indeterminate FRP-reinforced concrete structures because of the brittle nature of FRP and the absence of sufficient data in the literature. However, previous studies have reported moment redistribution in continuous beams reinforced with adequate FRP reinforcement at mid-span sections (El-Mogy et al. 2010). In this paper, test results of six continuous concrete slabs internally reinforced with basalt FRP (BFRP) bars are reported.

2. EXPERIMENTAL PROGRAM

2.1 Test Matrix

Six two-span continuous slab strips internally reinforced with BFRP bars were tested. Aiming to achieve two modes of failure (rupture of BFRP bars and crushing of concrete), the specimens were categorized into two groups [A] and [B] of three specimens each as demonstrated in Table 1. The sagging sections of specimens of group [A] were designed to be over-reinforced with $\rho_f = 2.5\rho_{fb}$ whereas those of specimens of group [B] were under-reinforced with $\rho_f = 0.8\rho_{fb}$, where ρ_f is the BFRP reinforcement ratio and ρ_{fb} is the BFRP balanced reinforcement ratio. Hogging regions are typically congested because of the use of excessive amount of reinforcement which might cause honeycombs and/or other defects during construction. If the hogging region section is of a sufficient ductility to make moment redistribution, the amount of reinforcement in the hogging region could be reduced provided increasing the reinforcement in the sagging regions. In such cases, hogging regions may have less amount of reinforcement than that of the sagging regions. The effect of varying the hogging-to-sagging reinforcement ratio on the moment redistribution capacity in continuous concrete structures internally reinforced with BFRP bars needs to be investigated. Accordingly, three different hogging-to-sagging BFRP reinforcement ratios of 0.5, 0.72, and 1 were used in the specimens of each group.

2.2 Specimens

Figure 1 shows a schematic of the beam specimen and the test set-up. The specimens were 500 mm wide, 200 mm deep and 5000 mm long. Each specimen had two clear spans of 2400 mm each. The beams were subjected to two point loads at $0.4L$ from the middle support, where L is the span length. To ensure a flexural mode of failure, double-leg steel stirrups of 8 mm diameter were provided along the length of the specimen at a spacing of 50 mm. The total applied load and the middle support reactions were recorded using 500-kN capacity load cells. Two linear variable differential transducers (LVDTs) were used to record the deflections under the point loads. Tests were conducted under displacement control at a rate of 1.5 mm/min. The specimens were constructed using ready-mixed normal weight concrete with average compressive and splitting strengths of 43 and 4.0 MPa, respectively. The BFRP reinforcing bars used were sand-coated with a nominal tensile strength of 1100 MPa and modulus of elasticity of 50.5 GPa. A test in progress is shown in Figure 2.

Table 1: Test matrix

Specimen	BFRP Reinforcing bars		Reinforcement ratio		Hogging-to-sagging reinforcement ratio
	Hogging	Sagging	Hogging ρ_f/ρ_{fb}	Sagging ρ_f/ρ_{fb}	
A1	1Φ10 + 2Φ12	2Φ10 + 4Φ12	1.25	2.5	0.5
A2	2Φ8 + 3Φ12	2Φ10 + 4Φ12	1.8	2.5	0.72
A3	2Φ10 + 4Φ12	2Φ10 + 4Φ12	2.5	2.5	1
B1	2Φ8	1Φ8 + 2Φ10	0.38	0.8	0.5
B2	3Φ8	1Φ8 + 2Φ10	0.58	0.8	0.72
B3	1Φ8 + 2Φ10	1Φ8 + 2Φ10	0.8	0.8	1

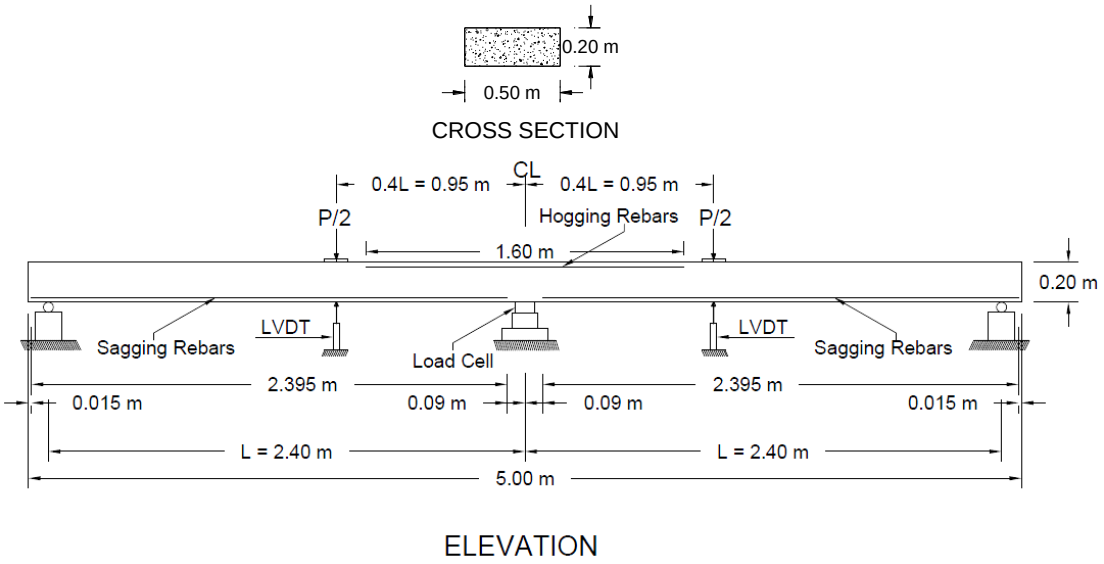

Figure 1: Test specimen and test set-up

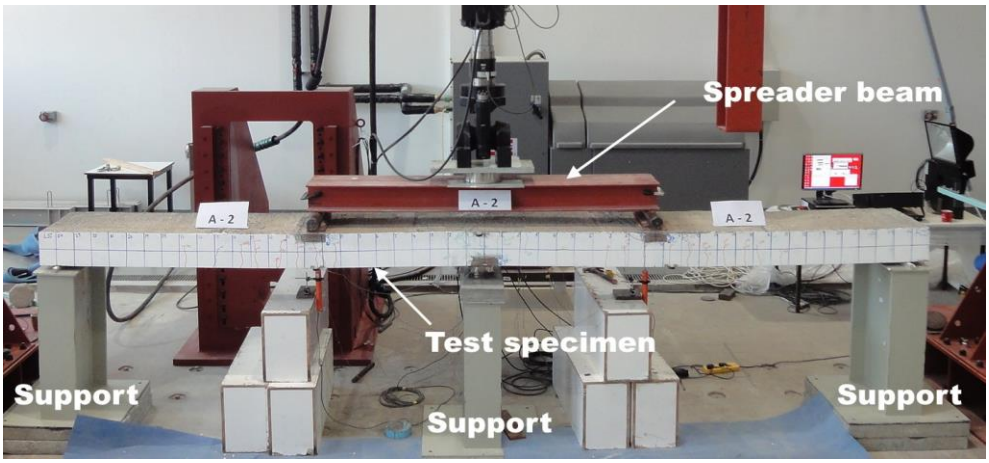

Figure 2: Test in Progress

3. TEST RESULTS AND DISCUSSION

3.1 Failure Mode

Specimens of group [A] initially exhibited flexural cracks in both sagging and hogging regions. As the load progressed, more flexural cracks developed in both regions. Prior to failure, an inclined flexure-shear crack developed in the hogging region. The specimens eventually failed by crushing of concrete in the hogging region over the middle support. Shortly after concrete crushing in the hogging region, the inclined flexure-shear crack widened and penetrated into the compression zone over the middle support, which caused a sudden collapse of the specimen. Local concrete crushing was also observed in the sagging regions at the onset of failure of specimen A3. Specimens of group [B] failed by rupture of the BFRP reinforcement in the hogging region after formation of several flexure cracks in both sagging and hogging regions. Rupture of BFRP bars resulted in a rapid release of energy and a complete loss of the load capacity of the beam. Figure 3 shows the modes of failure for specimens A1 and B3.

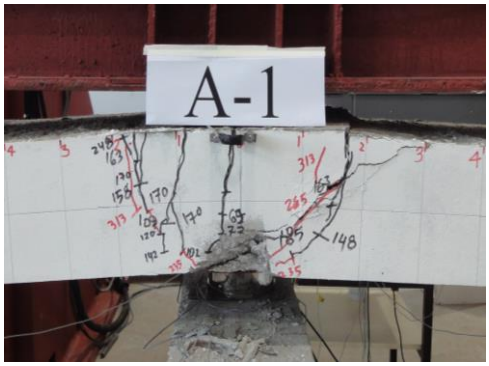

(a)

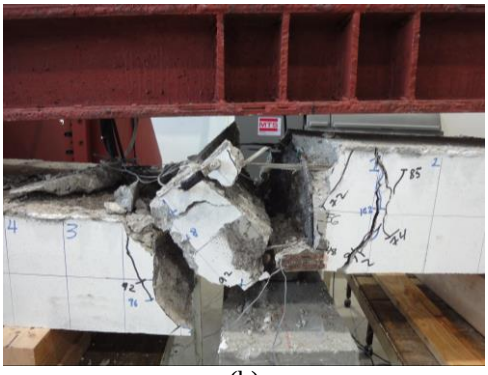

(b)

Figure 3: (a) Concrete crushing for specimen A1 and (b) BFRP rupture for specimen B3

3.2 Load-Deflection Response

The load-deflection response of the tested specimens is shown in Figure 4 whereas main test results are summarized in Table 2. Specimens of group [A] showed higher stiffness than that of specimens of group [B] in both the pre-cracking and the post-cracking stages. After cracking, the deflection increased at a higher rate in all specimens. The post-cracking stiffness was affected by the hogging-to-sagging BFRP reinforcement ratio. Increasing the hogging-to-sagging BFRP reinforcement ratio from 0.5 to 0.72 increased the post-cracking stiffness by 21% and 25% for specimens of groups [A] and [B], respectively. Further increase in the hogging-to-sagging BFRP reinforcement ratio from 0.72 to 1 had an almost no effect on the post-cracking stiffness.

From Table 2, it can be seen that, flexural cracks initiated earlier in specimens of group [B] than in those of group [A]. This occurred because specimens of group [B] had lower BFRP reinforcement ratios compared to those of group [A]. Varying the hogging-to-sagging BFRP reinforcement ratio had an almost no effect on the cracking load. Specimens of group [A] exhibited higher ultimate loads than those of group [B]. The load capacity typically increased in both groups with an increase in the hogging-to-sagging BFRP reinforcement ratio. The effect of varying the hogging-to-sagging BFRP reinforcement ratio on the load capacity was more pronounced in specimens of group [B] with the BFRP rupture mode of failure. Doubling the hogging-to-sagging BFRP reinforcement ratio increased the load capacity by 30% for specimens of group [B]. In contrast, specimens of group [A] exhibited only 18% increase in the load capacity as a result of doubling the hogging-to-sagging BFRP reinforcement ratio. It can then be concluded that the flexural response of continuous slabs with BFRP rupture mode of failure was more sensitive to the hogging-to-sagging BFRP reinforcement ratio than that of slabs with the concrete crushing mode failure. Specimens of group [A] featured higher deflection at peak load than that of specimens of group [B]. The deflection at peak typically increased by increasing the hogging-to-sagging BFRP reinforcement ratio. Doubling the hogging-to-sagging BFRP reinforcement ratio increased the deflection at peak by 10% for specimens of group [A] and 30% for those of group [B].

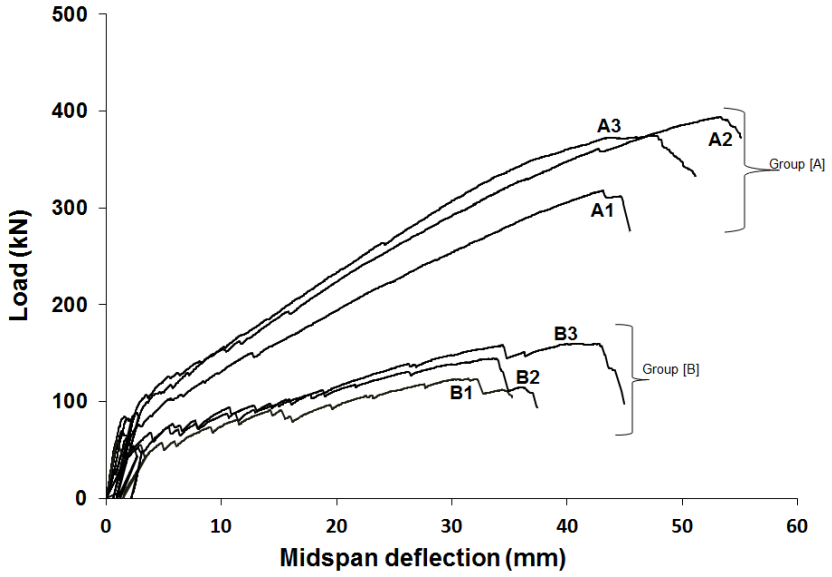

Figure 4: Load-deflection response

Table 2: Test results

Specimen	Cracking load, P_{cr} (kN)		Ultimate load, P_u (kN)	Deflection at peak, Δ_{Peak} (mm)	Mode of failure and its location
	Sagging	Hogging			
A1	67	67	317.6	43.12	CC[a] in hogging followed by SF[b] in hogging
A2	80	84	393.6	53.32	CC in hogging followed by CC in sagging
A3	80	82	374.6	47.16	CC in hogging with observed MC[c] in sagging
B1	55	58	123.5	31.45	BFRP rupture in hogging
B2	46	45	144	35.87	BFRP rupture in hogging
B3	50	59	160	40.72	BFRP rupture in hogging

[a] CC = Concrete crushing
[b] SF = Shear failure
[c] MC = Minor concrete crushing

3.3 Moment Redistribution

The load versus moment relationships for specimens of groups [A] and [B] are plotted in Figures 5 and 6, respectively. The moments were calculated based on satisfying the equilibrium conditions using values of the middle support reaction and total applied load. In the pre-cracking stage, the moments measured experimentally coincided with the predicted elastic moments. Following cracking, the moments started to deviate from the elastic response except for specimen B3 that featured an almost elastic response. This occurred because specimen B3 had same amount of BFRP reinforcement in both sagging and hogging regions. Specimen A1 from group [A] and B1 from group [B] exhibited the greatest deviation from the elastic response because they had the smallest hogging-to-sagging BFRP reinforcement ratio of 0.5. The deviation from the elastic response decreased with an increase in the hogging-to-sagging BFRP reinforcement ratio.

The moment redistribution ratio, β, of the tested specimens at ultimate load was calculated using Eq. 1 based on the difference between the moment obtained from the tests, M_{exp}, and the corresponding elastic moment, M_e. A positive

value of β indicates that the concerned region has gained a moment greater than the elastic moment whereas a negative value indicates the opposite. The moment redistribution ratio at ultimate in the sagging region was in the range of +40% to +48% for specimens of group [A] and +10% to +26% for specimens of group [B]. For specimens of group [A], the moment redistribution ratio at failure increased by increasing the hogging-to-sagging BFRP reinforcement ratio. This occurred because increasing the hogging-to-sagging BFRP reinforcement ratio increased the ultimate load, which allowed the slabs to develop more cracks, and hence, greater deviation from the elastic response occurred. In contrast, for specimens of group [B], the moment redistribution ratio at failure decreased by increasing the hogging-to-sagging BFRP reinforcement ratio. This occurred because increasing the hogging-to-sagging BFRP reinforcement ratio in specimens of group [B] reduced the difference in flexural rigidity between the sagging and hogging regions, and hence, reduced the moment redistribution at failure.

$$\beta\% = \frac{M_{exp} - M_e}{M_e} \times 100\% \quad (1)$$

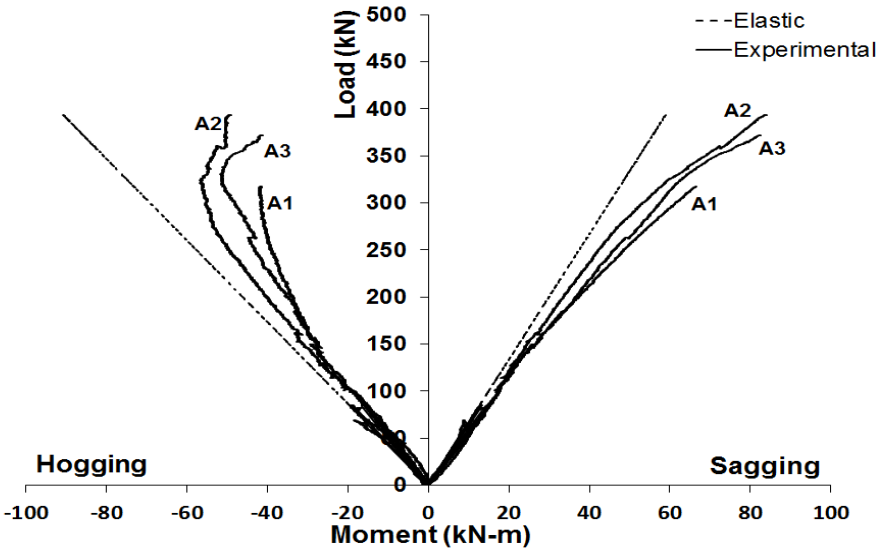

Figure 5: Load-moment response for specimens of group [A]

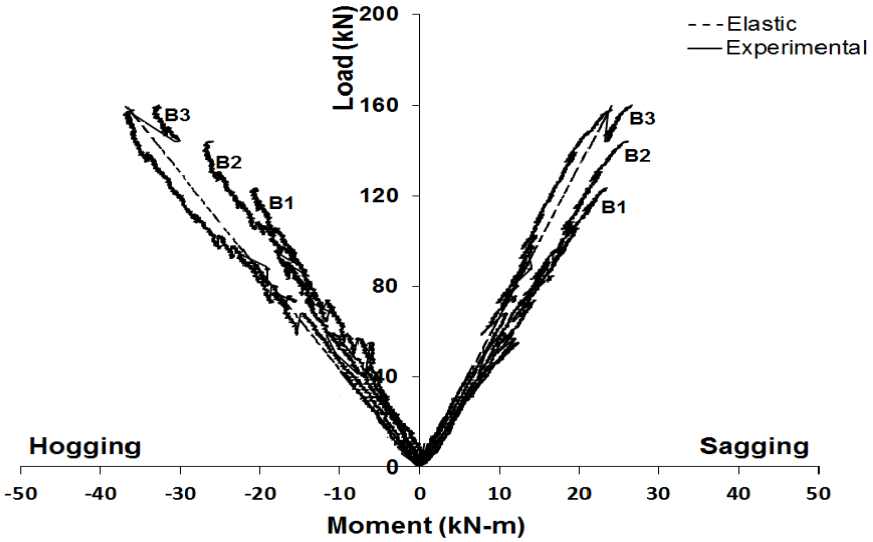

Figure 6: Load-moment response for specimens of group [B]

4. CONCLUSION

Increasing the hogging-to-sagging BFRP reinforcement ratio increased the ultimate load but had an almost no effect on the cracking load. The flexural response of continuous slabs with BFRP rupture mode of failure was more sensitive to the hogging-to-sagging BFRP reinforcement ratio than that of slabs with the concrete crushing mode of failure. Doubling the hogging-to-sagging BFRP reinforcement ratio increased the load capacity by 18% and 30% for specimens of groups [A] and [B] with concrete crushing and BFRP rupture modes of failure, respectively. Increasing the hogging-to-sagging BFRP reinforcement ratio from 0.5 to 0.72 increased the post-cracking stiffness. Further increase in the hogging-to-sagging BFRP reinforcement ratio from 0.72 to 1 had an almost no effect on the post-cracking stiffness. The moment redistribution ratio in the sagging region at failure was in the range of +40% to +48% for the specimens with a concrete crushing mode of failure and +10% to +26% for the specimens with a BFRP rupture mode of failure. The moment redistribution ratio at failure increased by increasing the hogging-to-sagging BFRP reinforcement ratio for the specimens with the concrete crushing mode of failure. In contrast, for specimens with the BFRP rupture mode of failure, the moment redistribution ratio at failure decreased by increasing the hogging-to-sagging BFRP reinforcement ratio.

ACKNOWLEDGMENTS

The authors would like to express their gratitude to the UAEU for financing this project under Grant No. 31N232.

5. REFERENCES

American Concrete Institute (ACI) 2006. Guide for the design and construction of concrete reinforced with FRP bars. *American Concrete Institute ACI 440.1R-06*, Farmington Hills, Michigan, USA.

Bank, L. 2006. *Composite for Construction: Structural design with FRP materials*, John Willey and Sons Ltd., USA.

Bakis, C., Bank, L., Brown, V.L., Cosenza, E., Davalos, J.F. Lesko, J.J., Machida, A., Rizkalla, S., and Triantafillou, T., 2002. Fiber-reinforced polymer composites for construction-state-of-the-art review. *Journal of Composites for Construction*, 6(2): 73–87.

El Maaddawy T., Soudki K., and Topper T., 2005a. Long-term performance of corrosion-damaged reinforced concrete beams. *ACI Structural Journal*, 102(5): 649–656.

El Maaddawy T., Soudki K., and Topper T., 2005b. Analytical model to predict nonlinear flexural behavior of corroded reinforced concrete beams. *ACI Structural Journal*, 102(4): 550–559.

El-Mogy, M., El-Ragaby A., and El-Salakawy E., 2010. Flexural behavior of continuous FRP-reinforced concrete beams. *Journal of Composites for Construction*, 14(6): 669–680.

Habeeb, M. and Ashour A., (2008). Flexural behavior of continuous GFRP reinforced concrete beams. *Journal of Composites for Construction*, 12(2): 115–124.

Kassem, C., Farghaly A., and Benmokrane B. 2011. Evaluation of flexural behavior and serviceability performance of concrete beams reinforced with FRP bars. *Journal of Composites for Construction*, 15(5): 682–695.

Ovitigala, T. and Issa M.A. 2013. Flexural behavior of concrete beams reinforced with basalt fiber reinforcement polymer (BFRP) Bars. *11th International Symposium on fiber reinforced polymers for reinforced concrete structures, FRPRCS-11*, Guimarães, Portugal.